XL CILAMCE
IBERO-LATIN AMERICAN CONGRESS ON COMPUTATIONAL METHODS IN ENGINEERING
NOVEMBER 11-14, 2019
Praiamar Natal Hotel & Convention
Natal, RN-BRAZIL

MULTI-OBJECTIVE TRUSS STRUCTURAL OPTIMIZATION CONSIDERING SIZE, SHAPE AND TOPOLOGY DESIGN VARIABLES SIMULTANEOUSLY

José Pedro Gonçalves Carvalho[1]
Afonso Celso de Castro Lemonge[2]
jose.carvalho@engenharia.ufjf.br
afonso.lemonge@ufjf.edu.br
[1]*Civil Engineering Program - Federal University of Rio de Janeiro*
Rua Horácio Macedo, Bloco G, 2030 - 101, 21941-450, Rio de Janeiro/RJ, Brazil
[2]*Department of applied and computational mechanics - Federal University of Juiz de Fora*
Rua José Lourenço Kelmer s/n, 36036-900, Juiz de Fora/MG, Brazil
Patrícia Habib Hallak[2]
Cláudio Horta Barbosa de Resende[3]
Beatriz de Souza Leite Pires de Lima[1]
patriciahallak@yahoo.com
claudio.horta@engenharia.ufjf.br
beatriz@poli.ufrj.br
[3]*Postgraduate Program of Civil Engineering - Federal University of Juiz de Fora*
Rua José Lourenço Kelmer s/n, 36036-900, Juiz de Fora/MG, Brazil

Abstract. Structural multi-objective optimization problems are common in real-world problems of Engineering field where one or more objective functions may be considered and desired to be optimized. In general, these functions are conflicting, leading to complex optimization problems. This paper analyses the multi-objective structural optimization problems considering the weight minimization (or volume) with the compliance or the maximum nodal displacement. The constraints refer to the allowable axial stresses in the bars. Several experiments are analyzed in this paper, presenting their Pareto-fronts showing the non-dominated solutions. The structural optimization problems consider sizing, shape, and topology design variables simultaneously, and they can be continuous, discrete, or mixed. One of the most important steps, after obtaining the Pareto curve, is the definition of which solution or solutions will be considered after obtaining the Pareto curve. This task is not trivial, and a Multi-Tournament Decision method is applied to extract the solutions from the Pareto based on Decision Maker preferences. The search algorithm adopted here is a modified version of the Differential Evolution called Third Evolution Step Differential Evolution (GDE3).

Keywords: Multi-objective Structural Optimization, Differential Evolution, Multi-Tournament Decision Method

1 INTRODUCTION

Structural optimization problems, common in engineering challenges, are often composed of conflicting objective functions, which leads to multi-objective optimization problems. For example, minimize the final weight of the structure is an opposite problem as minimize it's displacements since minimize the weight implies on stiffness loss. Independent of the nature of the optimization problem (mono or multi-objective), in almost all of them, there will always be constraints that must be satisfied (i.e., maximum displacements, maximum stresses, etc.).

Simultaneously sizing and shape optimization with static-related and dynamic-related constraints is a non-linear task that can leads to complicated and non-intuitive solutions. Including topology on this problems, the non-linearity and complexity rise significantly, leading to local optimum that can be seen on the Pareto fronts, i.e., these curves may be composed by multiple "sub-Pareto" that represents these different topologies.

This paper deals with sizing, shape, and topology simultaneously optimization on well-established structures found on literature. Most of these problems are based on mono-objective formulations and contemplates only static or dynamic-related constraints. In this sense, this work proposes as a novelty a multi-objective approach with both combined static and dynamic-related constraints. The results of the multi-objective optimization are analyzed via well-known metrics. A Multicriteria Tournament Decision (MTD) Method (proposed by Parreiras and Vasconcelos [1]) to extract the solutions from the Pareto fronts are adopted in this paper. The optimization algorithm used is the Differential Evolution (DE) (proposed by Kukkonen and Lampinen [2]) coupled to the Adaptative Penalty Method (APM) (proposed by Barbosa and Lemonge [3]).

Surveys of the latest developments considering meta-heuristics for solving structural design problems can be found in in Zavala et al. [4] and Barbosa et al. [5], respectively. In the following references detailed discussion on strategies, methods, approaches, formulations, etc, to solve multi-objective structural optimization with several type of objective functions and constraints are presented: Coello et al. [6], Kalyanmoy [7], Greiner et al. [8], Noilublao and Bureerat [9, 9], Greiner et al. [10], Su et al. [11], Richardson et al. [12], Greiner and Hajela [13], Kaveh and Laknejadi [14], Hosseini et al. [15], Angelo et al. [16], Assimi et al. [17], Tejani et al. [18], Mokarram and Banan [19], Vargas et al. [20], Tejani et al. [21], Kaveh and Mahdavi [22]. Remarking that this paper does not attempt to describe on details each one of these references.

The remainder of the paper is organized as follows: section 2 defines the multi-objective structural optimization Problem; section 3 presents a synthesis of the Third Evolution Step of Generalized Differential Evolution (GDE3) and the metrics used to evaluate the performance of the GDE3 are presented in section 4; a multicriteria decision making is used to define an extraction method of preferred solutions from the Pareto front and it is presented in Section 5; the computational experiments are discussed in Section 6, and, finally, the conclusions and future work are presented in Section 7.

2 MULTI-OBJECTIVE STRUCTURAL OPTIMIZATION PROBLEM

The multi-objective structural optimization problem presented in this paper refers to find a set of decision variables $\mathbf{x} = (x_1, \ldots, x_n)$, that correspond to the size, shape, and layout design variables of truss structures, and written as:

$$\begin{aligned} \min \quad & of_1(\mathbf{x}) \quad \text{and} \quad \max \quad of_2(\mathbf{x}) \\ \text{s.t.} \quad & \text{structural constraints} \end{aligned} \tag{1}$$

where $of_1(\mathbf{x})$ and $of_2(\mathbf{x})$ are the conflicting object functions, and the constraints are the maximum nodal displacements, axial stresses, natural frequencies of vibration or elastic critical loads concerning the global stability.

Three sets of computational experiments are discussed in this paper where the weight $W(\mathbf{x})$ of the structure is always the first objective function to be minimized and written as:

$$W(\mathbf{x}) = \sum_{i=1}^{N} \rho A_i L_i \tag{2}$$

where ρ is the specific mass of the material and A_i and L_i are the cross-sectional areas and the length of the i-th bar of the structure, respectively. The number of bars of the structure is denoted by N.

The sizing design variables are denoted by $\mathbf{x} = \{A_1, A_2, ..., A_N, X_i, Y_i, Z_i\}$, where A_i are the sizing design variables concerning the cross-sectional areas of the bars (continuous or discrete) and X_i, Y_i, Z_i are the shape design variables (continuous).

1. The first multi-objective truss structural optimization is written as:

$$\begin{aligned} \min \quad & W(\mathbf{x}) \quad \text{and} \quad \max \quad f_1(\mathbf{x}) \\ \text{s.t.} \quad & \sigma_i(\mathbf{x}) \leq \overline{\sigma} \\ & u_j(\mathbf{x}) \leq \overline{u} \\ & \lambda_1(\mathbf{x}) \geq \overline{\lambda} \end{aligned} \tag{3}$$

   where $f_1(\mathbf{x})$ is the first natural frequency of vibration, $\sigma_i(\mathbf{x})$ is the axial stress at the i-th bar, $u_j(\mathbf{x})$ is the displacement at the j-th node and $\lambda_1(\mathbf{x})$ is the smallest load factor with respect to the maximum elastic critical load able to be applied to the structure.

2. The second multi-objective truss structural optimization is written as:

$$\begin{aligned} \min \quad & W(\mathbf{x}) \quad \text{and} \quad \max \quad \lambda_1(\mathbf{x}) \\ \text{s.t.} \quad & \sigma_i(\mathbf{x}) \leq \overline{\sigma} \\ & u_j(\mathbf{x}) \leq \overline{u} \\ & f_1(\mathbf{x}) \geq \overline{f} \end{aligned} \tag{4}$$

   where $\lambda_1(\mathbf{x})$ is the smallest load factor with respect to the maximum elastic critical load able to be applied to the structure, $u_j(\mathbf{x})$ is the displacement at the j-th node and $f_1(\mathbf{x})$ is the first natural frequency of vibration.

3. The third multi-objective truss structural optimization is written as:

$$\begin{aligned} \min \quad & W(\mathbf{x}) \quad \text{and} \quad \min \quad u_{\max}(\mathbf{x}) \\ \text{s.t.} \quad & \sigma_i(\mathbf{x}) \leq \overline{\sigma} \\ & f_1(\mathbf{x}) \geq \overline{f} \\ & \lambda_1(\mathbf{x}) \geq \overline{\lambda} \end{aligned} \tag{5}$$

   where $u_{\max}(\mathbf{x})$ is the maximum nodal displacement of the structure, $\sigma_i(\mathbf{x})$ is the axial stress at the i-th bar and $\lambda_1(\mathbf{x})$ is the smallest load factor with respect to maximum elastic critical load able to be applied to the structure.

In the problem formulations the constraints are normalized , such as:

$$\frac{u_j(\mathbf{x})}{\bar{u}} - 1 \leq 0, \quad 1 \leq j \leq m_u, \tag{6}$$

$$\frac{\sigma_i(\mathbf{x})}{\bar{\sigma}} - 1 \leq 0, \quad 1 \leq i \leq m_\sigma, \tag{7}$$

$$1 - \frac{f_l(\mathbf{x})}{\bar{f}} \leq 0, \quad 1 \leq l \leq m_f \tag{8}$$

$$1 - \frac{\lambda_l(\mathbf{x})}{\bar{\lambda}} \leq 0, \quad 1 \leq l \leq m_\lambda \tag{9}$$

where m_u is the number of degree of freedom of the structure, $m_\sigma = N$ is the total number of bars, m_f is the total number of constrained natural frequencies of vibration and m_λ is the total number of constrained load factors of the structure. The allowable displacements, stresses, natural frequency of vibration and load factor are defined by $\bar{u}$, $\bar{\sigma}$, $\bar{f}$ and $\bar{\lambda}$, respectively.

The nodal displacements $\{u\}$ are obtained by the equilibrium equation for a discrete system of bars, which is written as:

$$[K]\{u\} = \{p\} \tag{10}$$

where $[K]$ is the stiffness matrix and $\{p\}$ are the load components Bathe [23].

The natural frequencies of vibration are obtained by the evaluation of the eigenvalues of the matrix

$$\left[(f_{m_f}^2 \times [M]) + [K]\right] \tag{11}$$

where $[M]$ is the mass matrix and f_{m_f} are the equivalent eigenvalues with respect to the m_f natural frequencies of the structure Bathe [23].

In the same way, the load factors λ concerning the global stability are obtained by the evaluation of the eigenvalues of the matrix

$$[[K] + \lambda_{m_\lambda}[K_G]] \tag{12}$$

where $[K_G]$ is the geometric matrix of the structure and λ_{m_λ} are the equivalent eigenvalues concerning the m_λ load factors of the structure. The lowest value λ_{cr} of λ_{m_λ} gives the buckling load factor or critical load factor for the structure (see McGuire et al. [24]).

3 THE THIRD EVOLUTION STEP OF GENERALIZED DIFFERENTIAL EVOLUTION (GDE3)

Differential Evolution (DE) was proposed by Storn and Price [25, 26] for single-objective optimization problems and The Third Evolution Step of Generalized Differential Evolution (GDE3), proposed by Kukkonen and Lampinen [2], extended the DE for constrained multi-objective optimization problems. The GDE3 starts randomly generating an initial population and improves it using DE's selection, mutation, and crossover operations. These steps are detailed bellow and use the crossover rate ($CR \in [0, 1]$), the mutation factor ($F \in \mathbb{R}$) and the population size (N) as parameters.

Let P_G be a population of N decision vectors $\mathbf{x}_{i,G}$ in generation G, where $i \in \{1, 2, 3, \ldots, N\}$ is a vector index. Each $\mathbf{x}_{i,G}$ of the population in generation G is a n-dimensional vector and $\mathbf{x}_{j,i,G}$ is its j-th component ($j \in \{1, 2, 3, \ldots, n\}$).

Then, a decision vector $\mathbf{x}_{i,G}$ creates the corresponding trial vector $\mathbf{u}_{i,G}$ through mutation and crossover operations Storn [27].

After the mutation and crossover operations, the trial vector $\mathbf{u}_{i,G}$ is compared to the decision vector $\mathbf{x}_{i,G}$ using the constraint domination concept. A vector $\mathbf{x}$ dominates a vector $\mathbf{y}$ (denoted by $\mathbf{x} \succeq_c \mathbf{y}$) if one, and only one, of the following conditions is true:

1. both are unfeasible and $\mathbf{x} \succ \mathbf{y}$ in the constraint function violation space.
2. $\mathbf{x}$ is feasible and $\mathbf{y}$ is unfeasible.
3. $\mathbf{x}$ and $\mathbf{y}$ are feasible and $\mathbf{x} \succ \mathbf{y}$ in the objective function space.

As a result, the trial vector $\mathbf{u}_{i,G}$ is selected to replace the decision vector $\mathbf{x}_{i,G}$ in the next generation P_{G+1} (population in generation $G + 1$) if $\mathbf{u}_{i,G} \succeq_c \mathbf{x}_{i,G}$. If $\mathbf{x}_{i,G} \succeq_c \mathbf{u}_{i,G}$, $\mathbf{u}_{i,G}$ is discarded and $\mathbf{x}_{i,G}$ remains in the population. Otherwise, both are included in P_{G+1}.

The size of the population is reduced using an elitist method when the size of P_{G+1} is greater than N. This elitist method in GDE3 is based on the Non-dominated Ranking and Crowding Distance, two

well-known schemes presented in NSGA-II (Deb et al. [28]). The Non-dominated Ranking scheme is used to define the non-domination levels and Crowding Distance is adopted to measure the diversity of solutions.

The size of the population P_{G+1} is reduced to N as follows: According to the Non-dominated Ranking scheme P_{G+1} is sorted, generating the sets $Rank_1, Rank_2, \ldots, Rank_d$, (i.e., $P_{G+1} = Rank_1 \cup Rank_2 \cup \cdots \cup Rank_d$). Given D, the smallest integer such that the size of the set $P_{aux} = Rank_1 \cup Rank_2 \cup \cdots \cup Rank_D$ is greater or equal to N. When D is equal to the size of P_{aux}, then $P_{G+1} = P_{aux}$. Otherwise, P_{G+1} is composed by the elements in P_{aux}, but after removing the candidate solutions from $Rank_D$ with the smallest Crowding Distance values until P_{G+1} has N elements. In both cases the solutions in $Rank_{D+1}, \ldots, Rank_d$ are discarded. More details on the Crowding Distance and the elitist method can be found in Vargas et al. [20], Deb et al. [29].

The Adaptive Penalty Method (APM) proposed by Barbosa and Lemonge [30] is adopted in this paper to handle the constraints. From the feedback of the evolutionary process, the method automatically sets a higher penalty coefficient on those constraints that seem to be more difficult to satisfy.

4 PERFORMANCE METRICS

It is often impossible to know the Pareto optimal set, in multi-objective optimization Nicoară [31]. There are several metrics proposed in the literature to evaluate the performance of a MOEAs, and some of them can be found in references Deb [32] Nicoară [31] Vargas et al. [33]. The performance metrics used in this paper are the Empirical Attainment Function and hypervolume. The notion of attainment function was first introduced by Fonseca and Fleming [34] and evaluates the distribution of a random non-dominated point by providing information about the probability of a given point is weakly dominated. This probability can be estimated from several runs of an algorithm. The EAF can be estimated as Grunert da Fonseca et al. [35].

$$\alpha_n(z) = \frac{1}{n} \sum_{i=1}^{n} b_i(z) \tag{13}$$

where $z \in \mathbb{R}^d$ and $b_1(z), ..., b_n(z)$ are n realizations of the attainment indicator $b_x(z)$.

In López-Ibánez et al. [36] is developed a tool for graphical analysis of the EAF[3]. Figure 1 shows three EAF curves (best, median, and worst cases) obtained by 10 independent runs of a given MOEA on a problem for two objective functions Carvalho et al. [37]. The best curve delimits the region dominated by all non-dominated solutions obtained in the 10 runs. The median EAF curve represents 50% of the attainment surface. Finally, the worst curve bounds the region dominated by any non-dominated solution found by the search technique in the 10 runs. Details about EAF code can be found in Fonseca and Fleming [34] and Coello et al. [6].

The Hypervolume (Zitzler and Thiele [38]) provides a qualitative measure of convergence as well as diversity in a combined sense. It allows an easy comparison between the results of different multi-objective algorithms, by assigning a real value to a set of points. Mathematically, according to (Deb [32]), for each solution $i \in Q$, a hypercube v_i is obtained with a reference point W and the solution i as the diagonal corners of the hypercube. The reference point can simply be found by constructing a vector of worst objective function values. Thereafter, an union of all hypercubes is found and its hypervolume (HV) is calculated

$$\text{HV} = \text{volume}\ (\cup_{i=1}^{|Q|} v_i) \tag{14}$$

[3] http://lopez-ibanez.eu/eaftools

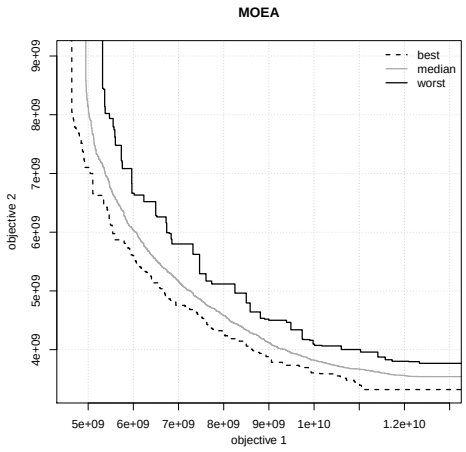

Figure 1. Example of the EAF curves (best, median and worst cases) Carvalho et al. [37]

5 THE MULTICRITERIA DECISION MAKING

After obtaining the Pareto fronts, a nontrivial task refers to the choice of which solution should be selected by the Decision Maker (DM). One way to do this, for example, is the definition of a preference interval that can even be explored in a new multi-objective analysis in this range.

However, it is possible to establish criteria defining weights (importance) for each objective and through these values, establish comparison scenarios (Parreiras and Vasconcelos [1], Angelo et al. [16]). On the other hand, the definition of these weights may also not be a trivial task Zhang et al. [39]. Although it is possible to use a strategy capable of indicating the preferred solutions from the weights defined by the DM. In this paper a Multicriteria Decision Maker (MCDM) is adopted to illustrate different scenarios defined by the DM to extract solutions from the Pareto frontier.

According to their objectives and preferences (weights) established by the Decision Maker, the MCDM establishes a Multi Tournament Decision Method which is a tournament-based method that ranks the best and the worst possible solutions in the Pareto frontier In this sense, a function $R(a)$ is introduced returning a global metric or preference of solution a when compared with others in the Pareto. It is necessary to give a criterion defined by the DM, and each solution is compared to the others in the Pareto front, by definition of the function $R(a)$. After that, a tournament is performed introducing a function $t_i(\alpha, A)$ that returns the number of times that solution a wins the tournament when compared with another solution b, where A is the whole set of solutions of the Pareto. The function $T_i(\alpha, A)$ is written as:

$$T_i(\alpha, A) = \sum_{\forall b \in A, a \neq b} \frac{t_i(a, b)}{(|A| - 1)}, \tag{15}$$

where $t_i(a, b)$ is given by:

$$t_i(a, b) = \begin{cases} 1, & \text{if } f_i(b) - f_i(a) > 0, \\ 0, & \text{otherwise} \end{cases} \tag{16}$$

After the tournament, each solution has indicators such as scores provided by function $T_i(a, A)$ informing its performance compared to the other solutions of set A. These scores are aggregated in the ranking $R(\cdot)$ considering all the criteria and their respective weights w_i, where Zhang et al. [39]:

$$R(a) = \left(\prod_{i=1}^{m} T_i(a, A)^{w_i} \right)^{1/m} \tag{17}$$

$$R(a) = \min\left[T_i(a, A)^{w_1}, \cdots, T_i(a, A)^{w_m}\right] \tag{18}$$

The values for each w_i have to be set by the DM according to the importance defined for each one, where $w_i > 0$ for $i = 1, \cdots, m$, and $\sum_{i=1}^{m} w_i = 1$. The scores defined by $R(a)$ provide a measure of preference of a solution a in comparison with a solution b, such as:

- if $R(a)$ > R(b), then a is preferred to b;
- if $R(a)$ = R(b), then a is indifferent to b;

A pseudo-code for this tournament-based method is presented in Parreiras and Vasconcelos [1].

6 COMPUTATIONAL EXPERIMENTS

In this section, two well-know truss structures found in the literature are analyzed: the 10-bar and the 52-bar. Results of the multi-objective optimization, as well as extraction of desired structures from Pareto fronts, are presented. Information about mesh, materials, and boundary conditions for each truss are found in respective problem's definitions.

Regarding the MTD extraction methodology, three scenarios are defined:

- s1 : w_1=0.3 and w_2=0.7 (meaning that Decision Maker sets 30% of importance to the first objective function and 70% of importance to the second objective function);
- s2: w_1=0.5 and w_2=0.5 (meaning that Decision Maker sets equal 50% of importance to both of the objective functions);
- s3: w_1=0.7 and w_2=0.3 (meaning that Decision Maker sets 70% of importance to the first objective function and 30% of importance to the second objective function);

6.1 The 10-bar truss

This experiment is a well-known problem found in literature corresponding to the 10-bar truss shown in Fig. 2. For this experiment, 10 sizing design variables are considered corresponding to each cross-sectional area of the bars, with values varying continuously from 0 to 33.5 in ^{2}. For shape optimization, nodal coordinates of nodes 1, 3, and 5 are free to move between 180 and 1000 in, leading to 3 shape design variables. Therefore, there is a total of 13 design variables. A nonstructural mass of 1000 lbs is attached at each free node.

When the natural frequencies are set as constraints, the limits are $f_1 \geq 7$ Hz, $f_2 \geq 15$ Hz and $f_3 \geq 20$ Hz. For nodal displacements, the maximum allowable value is equal to 2 in. For stability analysis, the minimum elastic critical load factor must be greater than 1.0. Also, there are constraints for stresses on the bars: both tension or compression stresses of each bar are bounded by 25 ksi. The density of the material is 0.1 lb/in^3, Young's modulus is E = 10^4 ksi and vertical downward loads of 100 kips are applied at nodes 2 and 4.

For the multi-objective structural optimization problem, 3 cases are considered:

- $\#1$ - weight minimization along with the sum of the first three natural natural frequencies of vibration;
- $\#2$ - weight minimization along with maximum nodal displacement minimization;
- $\#3$ - weight minimization along with elastic critical load maximization;

The obtained Pareto curves are shown in Figures 3 to 5 and corresponding EAF's and hypervolumes are shown in Figures 6 to 8. Figure 9 shows the Pareto fronts for the three cases analyzed in the 10-bar truss, at left sides, and right sides, their respective extracted solutions according to the preferences of the Decision Maker. Table 1 shows the design variables and constraints of the solutions of the 10-bar truss extracted from Pareto fronts according to MTD Method.

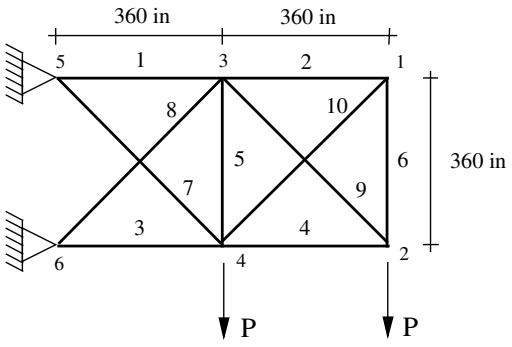

Figure 2. The 10-bar truss.

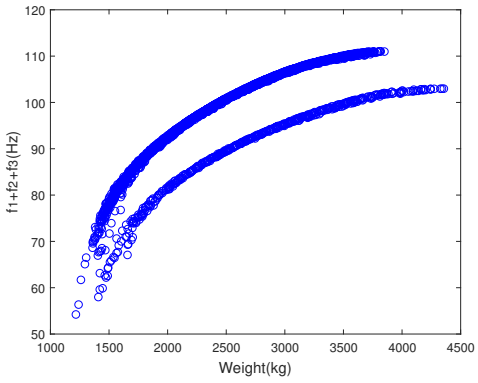

Figure 3. Pareto obtained for case #1 of the 10-bar truss.

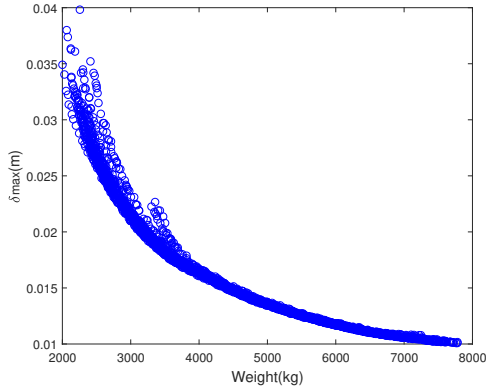

Figure 4. Pareto obtained for case #2 of the 10-bar truss.

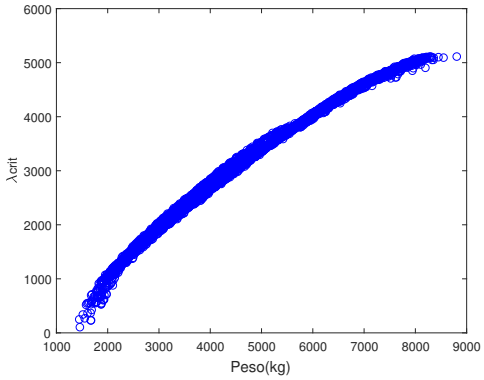

Figure 5. Pareto obtained for case #3 of 10-bar truss.

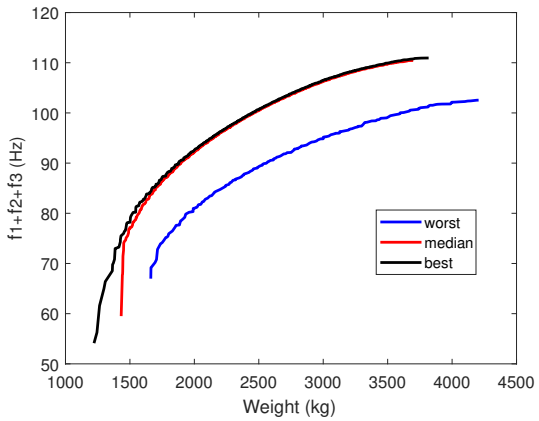

Figure 6. EAF obtained for case #1 of 10-bar truss, HV_{best} = 1, HV_{median} = 0.97274 and HV_{worst} = 0.72539.

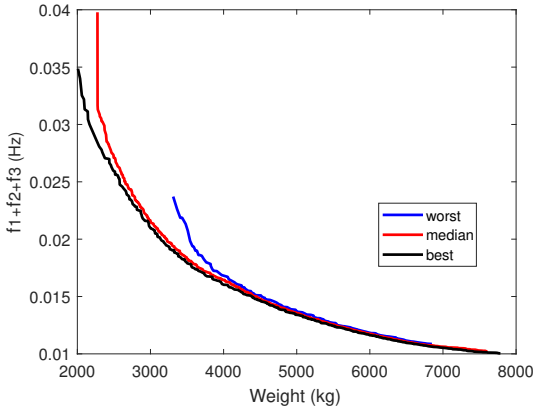

Figure 7. EAF obtained for case #2 of 10-bar truss, HV_{best} = 1, HV_{median} = 0.97158 and HV_{worst} = 0.83968.

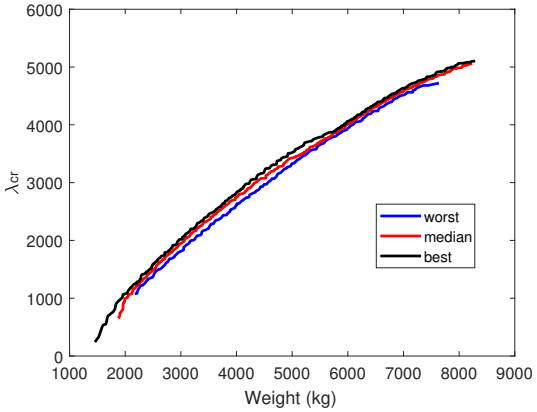

Figure 8. EAF obtained for case #3 of 10-bar truss, HV_{best} = 1, HV_{median} = 0.97063 and HV_{worst} = 0.92475.

Table 1. Design variables and constraints of the solutions of 10-bar truss extracted from Pareto fronts according to MTD Method. The cross-sectional A_i are given in cm^2 and Y_i coordinates are given in meters.

	Case								
	1			2			3		
	Scenario			Scenario			Scenario		
dv	1	2	3	1	2	3	1	2	3
A_1	216.1286	174.6373	148.9833	216.1286	216.1286	212.7174	176.5309	165.3551	117.1051
A_2	0	0	0	127.7941	71.8631	0	152.0380	138.5101	105.0163
A_3	216.1286	206.0584	167.6150	216.1286	216.1286	196.5068	88.4451	70.6855	54.1171
A_4	101.0610	103.8380	89.0969	108.9810	138.5372	118.8616	126.0261	107.3537	86.8536
A_5	59.5559	53.6408	45.5316	0	0	0	216.1286	210.3947	216.1286
A_6	0	0	0	140.3939	78.4830	0	46.6174	49.1892	52.0334
A_7	92.2709	90.6950	75.2890	183.8183	158.2582	101.4447	0	0	0
A_8	171.9056	135.1967	96.7983	119.6030	117.4986	72.6833	200.0035	143.5753	97.7919
A_9	100.8641	89.3689	82.1227	215.5695	216.1286	211.1505	1.2613	1.2371	1.5736
A_{10}	0	0	0	72.0647	43.7972	0	216.1286	215.7627	157.2009
Y_1	-	-	-	4.5720	4.5720	-	17.0100	15.7189	13.1602
Y_3	6.8668	7.5424	8.5648	16.4487	15.6224	13.0746	19.5962	18.0858	17.2902
Y_5	11.3710	11.6358	12.7233	24.2899	22.8190	20.5424	25.4000	25.4000	25.3802
Objective functions & constraints									
Weight (kg)	2761	2488	2118	5520	4849	3377	5222	4513	3502
f_1 (Hz)	27.64	27.55	27.89	24.68	25.66	26.61	17.18	17.30	17.62
f_2 (Hz)	51.65	51.32	50.19	33.77	34.76	34.54	29.90	27.73	26.35
f_3 (Hz)	70.73	68.19	64.59	35.70	39.88	43.03	34.59	32.33	30.62
λ_{cr}	393	390	375	794	633	308	3691	3232	2457
u_{max} (cm)	5.04	5.07	5.08	1.24	1.37	1.87	5.05	4.91	4.89
σ_{max} (MPa)	73.63	78.41	78.43	28.26	32.19	48.11	111.67	107.88	94.06

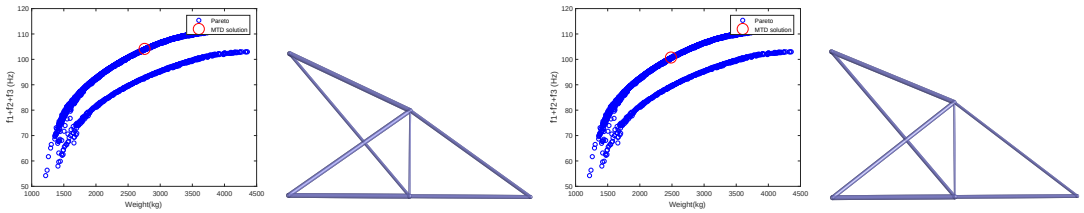

a Case #1, w=0.3 0.7

c Case #1, w=0.5 0.5

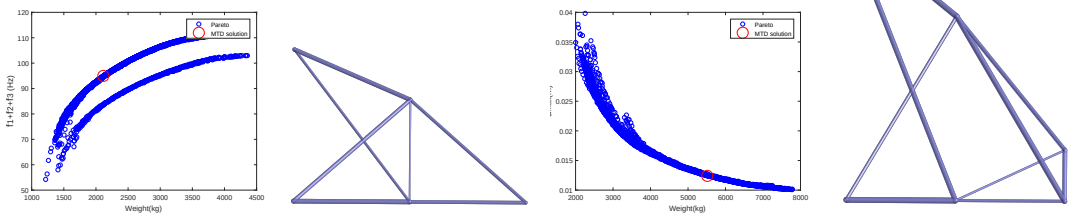

e Case #1, w=0.7 0.3

g Case #2, w=0.3 0.7

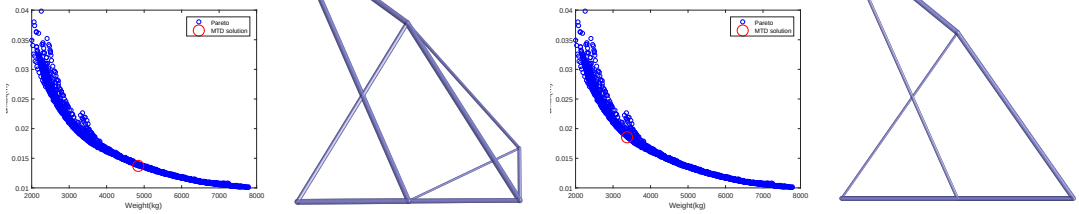

i Case #2, w=0.5 0.5

k Case #2, w=0.7 0.3

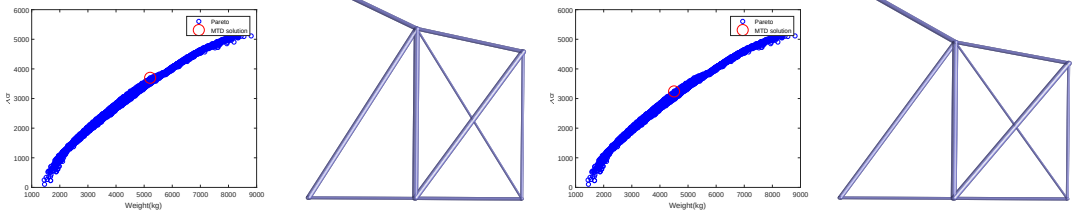

m Case #3, w=0.3 0.7

o Case #3, w=0.5 0.5

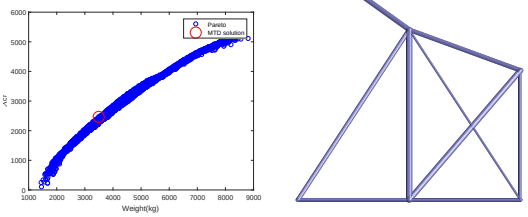

q Case #3, w=0.7 0.3

Figure 9. Pareto fronts for the three cases analyzed in the 10-bar truss, at left sides, and at right sides, their respective extracted solutions according to the preferences of the Decision Maker.

6.2 The 52-bar truss dome

This next experiment corresponds to the multi-objective structural optimization of the 52-bar truss dome depicted in Figures 10 and 11. The material has Young's modulus E = 210 GPa and density ρ = 7800 kg/m^3 and a nonstructural mass of 50 kg is attached at all free nodes. For sizing optimization, the cross-sectional areas are linked in 8 groups: $A_1 - A_4$, $A_5 - A_8$, $A_9 - A_{16}$, $A_{17} - A_{20}$, $A_{21} - A_{28}$, $A_{29} - A_{36}$, $A_{37} - A_{44}$ and $A_{45} - A_{52}$ (according to the symmetry around the central node); for shape optimization, nodal coordinates are free to move between $\pm$ 2.0 me :x_2, x_6, z_2, z_6 and z_1 (also keeping the symmetry for all nodes). Therefore, there is a total of 13 design variables (8 for sizing and 5 for shape). The search space for sizing design variables is composed of the continuous space between 0 and 10.0 cm^2.

Again, it is considered the same idea for the 3 cases introduced in the 10-bar truss:

- #1 - weight minimization along with maximization of the first natural frequency of vibration;
- #2 - weight minimization along with maximum nodal displacement minimization;
- #3 - weight minimization along with elastic critical load maximization;

When natural frequencies of vibrations are set as constraints, the limits are $f_1 \leq$ 15.9155 Hz and $f_2 \geq$ 28.6479 Hz; for nodal displacements, the maximum allowable value is equal to 0.04 m (4 cm); for stability analysis, the minimum elastic critical load factor must be greater than 1.0. Also, there are constraints for axial stress in the bars: both tension or compression stresses of each bar are bounded by 172.37 MPa. The vertical downwards loads are 1000 kN at node 1, 2500 kN at nodes 2-5 and 1250 kN at nodes 6-13.

The obtained Pareto curves are shown in Figures 12 to 14 and corresponding EAF's and hypervolumes are shown in Figures 15 to 17. Figure 18 shows the Pareto fronts for the three cases analyzed in the 52-bar truss, at left sides, and right sides, their respective extracted solutions according to the preferences of the Decision Maker. Table Table 2 shows the design variables and constraints of the solutions of the 52-bar truss dome extracted from Pareto fronts according to MTD Method.

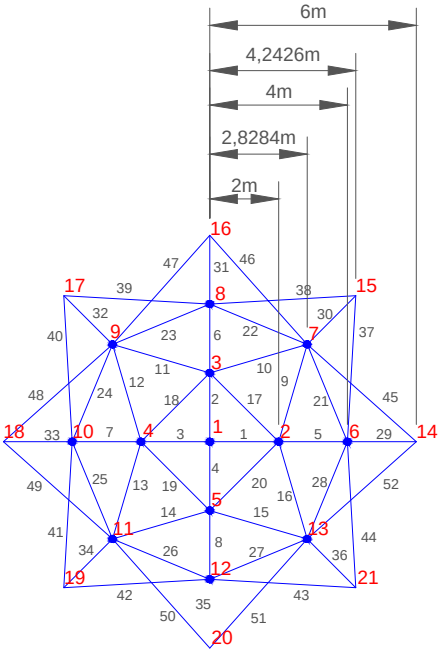

Figure 10. The 52-bar truss dome – top view.

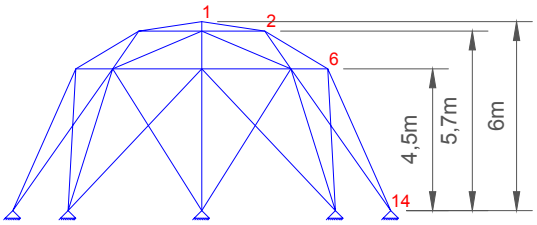

Figure 11. The 52-bar truss dome – side view.

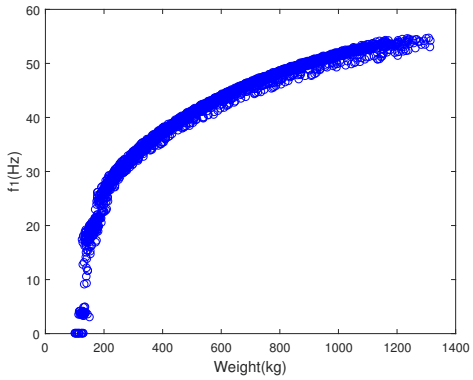

Figure 12. Pareto obtained for case #1 of t52.

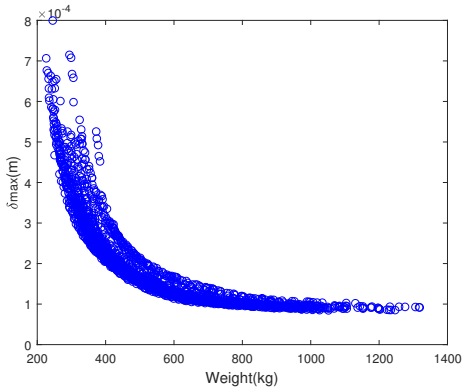

Figure 13. Pareto obtained for case #2 of t52.

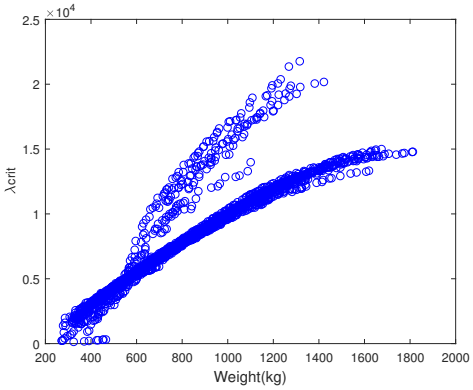

Figure 14. Pareto obtained for case #3 of t52.

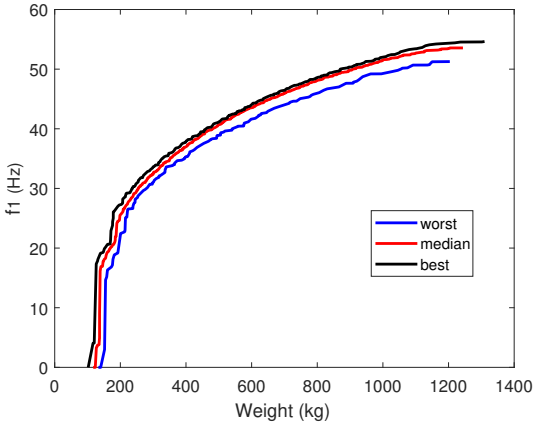

Figure 15. EAF obtained for case #1 of t52, HV_{best} = 1, HV_{median} = 0.97859 and HV_{worst} = 0.92606.

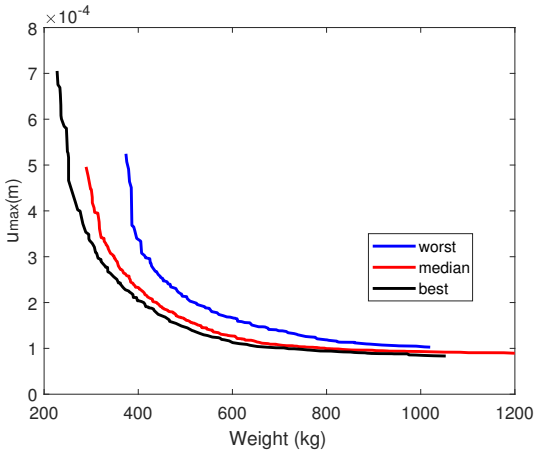

Figure 16. EAF obtained for case #2 of t52, HV_{best} = 1, HV_{median} = 0.95082 and HV_{worst} = 0.84481.

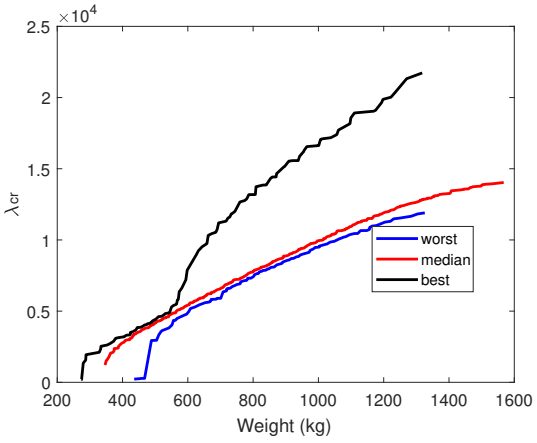

Figure 17. EAF obtained for case #3 of t52, HV_{best} = 1, HV_{median} = 0.61377 and HV_{worst} = 0.54187.

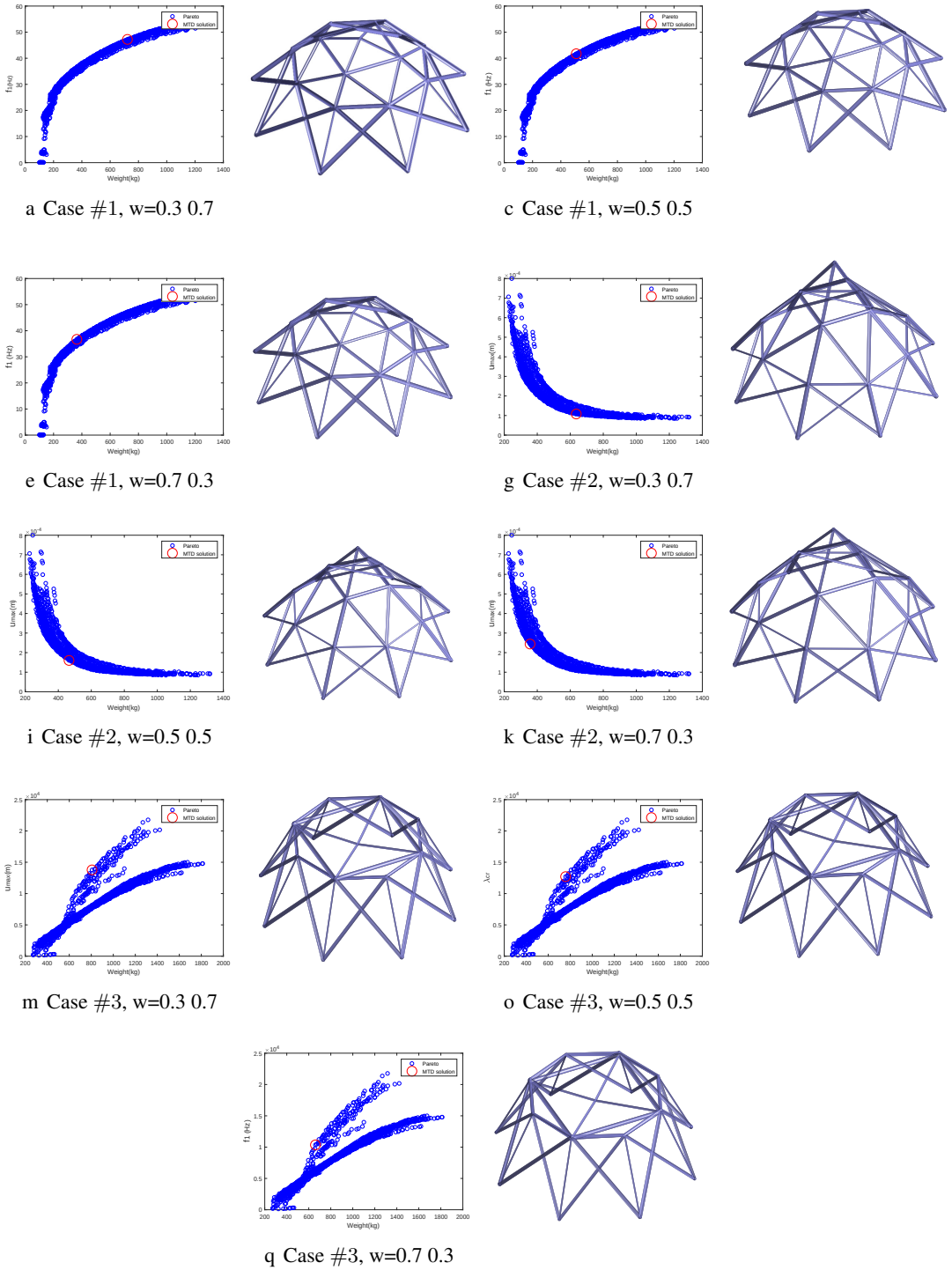

a Case #1, w=0.3 0.7 c Case #1, w=0.5 0.5

e Case #1, w=0.7 0.3 g Case #2, w=0.3 0.7

i Case #2, w=0.5 0.5 k Case #2, w=0.7 0.3

m Case #3, w=0.3 0.7 o Case #3, w=0.5 0.5

q Case #3, w=0.7 0.3

Figure 18. Pareto fronts for the three cases analyzed in the 52-bar truss dome, at left sides, and at right sides, their respective extracted solutions according to the preferences of the Decision Maker

Table 2. Design variables and constraints of the solutions of the 52-bar truss dome extracted from Pareto fronts according to MTD Method. The cross-sectional areas A_i are given in cm^2 and X_i and Z_i coordinates are given in meters.

	Case								
	1			2			3		
	Scenario			Scenario			Scenario		
dv	1	2	3	1	2	3	1	2	3
A_1	4.0636	3.2232	2.2111	4.0706	2.5046	1.5534	2.6533	2.7549	2.3778
A_2	4.3495	4.1591	2.4446	10.0000	8.0210	4.3892	4.5708	8.0463	6.2896
A_3	4.2898	3.2238	2.4185	4.5321	2.8793	2.2170	3.1670	3.1961	2.9383
A_4	4.3087	3.3474	2.3176	5.1453	4.0900	2.2679	9.5539	8.9232	8.0963
A_5	5.1198	3.6578	2.6529	1.2648	1.0663	1.2349	3.5930	2.8938	3.3799
A_6	1.8548	1.4153	1.1582	10.0000	6.8681	4.8151	1.1367	1.1595	1.1501
A_7	6.2858	4.1652	2.7783	2.2919	2.3072	1.9288	6.6151	7.2411	5.4386
A_8	6.8928	4.6207	3.3836	1.1964	1.1750	1.3936	4.9026	3.5020	3.2629
Z_1	4.54	4.41	4.63	7.99	7.11	7.6840	4.0714	4.0174	4.0819
X_2	2.25	2.20	2.18	2.08	2.01	2.4348	3.9346	3.9677	3.9348
Z_2	3.86	3.80	3.97	5.09	4.68	4.8591	4.5161	4.4299	4.3794
X_6	3.77	3.80	3.78	4.29	4.11	4.3881	3.9266	3.9530	3.9459
Z_6	2.73	2.65	2.77	2.51	2.51	2.5234	4.5516	4.5196	4.4969
Objective functions & constraints									
Weight (kg)	723.89	510.54	366.12	637.61	466.45	357.73	808.86	759.58	662.46
f_1 (Hz)	47.14	41.64	36.61	15.39	15.49	15.70	15.61	14.42	10.03
f_2 (Hz)	47.17	41.64	36.74	29.04	28.81	29.24	30.75	29.28	29.37
λ_{cr}	1524	1124	880	445	323	348	13739	12667	10322
u_{max} (cm)	0.04	0.04	0.06	0.01	0.02	0.02	0.19	0.22	0.44
σ_{max} (MPa)	6.94	10.34	13.06	2.96	4.30	6.07	8.39	8.78	13.94

7 CONCLUSIONS AND FUTURE WORK

One can observe that some of the Pareto curves were not ' "unique"; the consideration design variables concerning topology optimization in these problems leads in a highly complex non-linear problem to be solved, having a significant effect on solutions found by the algorithm: there are bifurcations on Pareto fronts representing these different topologies found by different independent runs, indicating a local minimum found in these runs. In a general conclusion, the obtained Pareto front for the both experiments were intuitive and coherent when compared to the same problems under mono-objective analysis performed in (Carvalho et al. [40], Souze et al. [41], Rahami et al. [42]), Vu [43].

Extracted solutions from MTD method showed a few different topologies. Again the results obtained were graphically intuitive when the preferred weights w_i for the objective functions are modified.

The experiments analyzed in this paper are considered small -scale, and the purpose is to offer a methodology that provides a range for the mono-objective problems found in the literature

For future works, it is intended to discuss large-scale multi-objective structural optimization problems (including *ground-structures*) to investigate more effectively the effects of the topology optimization, also considering new objective functions. It is expected to analyze the same experiments modeling the structures as 3D frames to investigate the different behavior.

Acknowledgements

This study was financed in part by the Coordenação de Aperfeiçoamento de Pessoal de Nível Superior - Brasil (CAPES) - Finance Code 001. The authors also thank the Graduate Program in Civil Engineering (UFJF) and Brazilian Agency CNPq (grant 306186/2017-9).

References

[1] Parreiras, R. & Vasconcelos, J., 2009. Decision making in multiobjective optimization aided by the multicriteria tournament decision method. *Nonlinear Analysis: Theory, Methods & Applications*, vol. 71, n. 12, pp. e191–e198.

[2] Kukkonen, S. & Lampinen, J., 2005. GDE3: The third evolution step of generalized differential evolution. In *IEEE Congress on Evolutionary Computation (CEC 2005)*, pp. 443–450. IEEE.

[3] Barbosa, H. J. C. & Lemonge, A. C. C., 2002a. An adaptive penalty scheme in genetic algorithms for constrained optimization problems. In *GECCO'02: Proceedings of the Genetic and Evolutionary Computation Conference.*, pp. 287–294, New York.

[4] Zavala, G. R., Nebro, A. J., Luna, F., & Coello, C. A. C., 2014. A survey of multi-objective metaheuristics applied to structural optimization. *Structural and Multidisciplinary Optimization*, vol. 49, n. 4, pp. 537–558.

[5] Barbosa, H. J. C., Bernardino, H. S., & Angelo, J. S., 2015. Derivative-free techniques for multiobjective structural optimization: A review. *Computational Technology Reviews*, vol. 12, pp. 27–52.

[6] Coello, C. A. C., Lamont, G. B., Van Veldhuizen, D. A., et al., 2007. *Evolutionary algorithms for solving multi-objective problems*, volume 5. Springer.

[7] Kalyanmoy, D., 2014. Multi-objective optimization. In *Search methodologies*, pp. 403–449. Springer.

[8] Greiner, D., Winter, G., Emperador, J. M., & Galván, B., 2005. Gray coding in evolutionary multicriteria optimization: application in frame structural optimum design. In *International Conference on Evolutionary Multi-Criterion Optimization*, pp. 576–591. Springer.

[9] Noilublao, N. & Bureerat, S., 2011. Simultaneous topology, shape and sizing optimisation of a three-dimensional slender truss tower using multiobjective evolutionary algorithms. *Computers & Structures*, vol. 89, n. 23-24, pp. 2531–2538.

[10] Greiner, D., Galván, B., Emperador, J. M., Méndez, M., & Winter, G., 2011. Introducing reference point using g-dominance in optimum design considering uncertainties: an application in structural engineering. In *International Conference on Evolutionary Multi-Criterion Optimization*, pp. 389–403. Springer.

[11] Su, R., Wang, X., Gui, L., & Fan, Z., 2011. Multi-objective topology and sizing optimization of truss structures based on adaptive multi-island search strategy. *Structural and Multidisciplinary Optimization*, vol. 43, n. 2, pp. 275–286.

[12] Richardson, J. N., Adriaenssens, S., Bouillard, P., & Coelho, R. F., 2012. Multiobjective topology optimization of truss structures with kinematic stability repair. *Structural and multidisciplinary optimization*, vol. 46, n. 4, pp. 513–532.

[13] Greiner, D. & Hajela, P., 2012. Truss topology optimization for mass and reliability considerations—co-evolutionary multiobjective formulations. *Structural and Multidisciplinary Optimization*, vol. 45, n. 4, pp. 589–613.

[14] Kaveh, A. & Laknejadi, K., 2013. A hybrid evolutionary graph-based multi-objective algorithm for layout optimization of truss structures. *Acta Mechanica*, vol. 224, n. 2, pp. 343–364.

[15] Hosseini, S. S., Hamidi, S. A., Mansuri, M., & Ghoddosian, A., 2015. Multi objective particle swarm optimization (mopso) for size and shape optimization of 2d truss structures. *Periodica Polytechnica Civil Engineering*, vol. 59, n. 1, pp. 9–14.

[16] Angelo, J. S., Bernardino, H. S., & Barbosa, H. J., 2015. Ant colony approaches for multiobjective structural optimization problems with a cardinality constraint. *Advances in Engineering Software*, vol. 80, pp. 101–115.

[17] Assimi, H., Jamali, A., & Nariman-zadeh, N., 2018. Multi-objective sizing and topology optimization of truss structures using genetic programming based on a new adaptive mutant operator. *Neural Computing and Applications*, pp. 1–21.

[18] Tejani, G. G., Pholdee, N., Bureerat, S., & Prayogo, D., 2018. Multiobjective adaptive symbiotic organisms search for truss optimization problems. *Knowledge-Based Systems*, vol. 161, pp. 398–414.

[19] Mokarram, V. & Banan, M. R., 2018. An improved multi-objective optimization approach for performance-based design of structures using nonlinear time-history analyses. *Applied Soft Computing*, vol. 73, pp. 647–665.

[20] Vargas, D. E., Lemonge, A. C., Barbosa, H. J., & Bernardino, H. S., 2019. Differential evolution with the adaptive penalty method for structural multi-objective optimization. *Optimization and Engineering*, vol. 20, n. 1, pp. 65–88.

[21] Tejani, G. G., Pholdee, N., Bureerat, S., Prayogo, D., & Gandomi, A. H., 2019. Structural optimization using multi-objective modified adaptive symbiotic organisms search. *Expert Systems with Applications*, vol. 125, pp. 425–441.

[22] Kaveh, A. & Mahdavi, V. R., 2019. Multi-objective colliding bodies optimization algorithm for design of trusses. *Journal of Computational Design and Engineering*, vol. 6, n. 1, pp. 49–59.

[23] Bathe, K.-J., 2006. *Finite element procedures*. Prentice Hall, Pearson Education, Inc.

[24] McGuire, W., Gallagher, R. H., & Ziemian, R. D., 2014. *Matrix structural analysis*. John Wiley & Sons, New York. 2nd Edition.

[25] Storn, R. & Price, K., 1995. Differential evolution a simple and efficient adaptive scheme for global optimization over continuous spaces. Tech. Rep. 95-012, Univ. of California, Berkeley, CA.

[26] Storn, R. & Price, K., 1997. Differential evolution a simple and efficient adaptive scheme for global optimization over continuous spaces. *Journal of Global Optimization*, vol. 11(4), pp. 341–359.

[27] Storn, R., 1995. Differrential evolution-a simple and efficient adaptive scheme for global optimization over continuous spaces. *Technical Report, International Computer Science Institute*, vol. 11.

[28] Deb, K., Pratap, A., Agarwal, S., & Meyarivan, T., 2002a. A fast and elitist multiobjective genetic algorithm: NSGA-II. *IEEE Transactions on Evolutionary Computation*, vol. 2(6), pp. 182–197.

[29] Deb, K., Pratap, A., Agarwal, S., & Meyarivan, T., 2002b. A fast and elitist multiobjective genetic algorithm: NSGA-II. *IEEE transactions on evolutionary computation*, vol. 6, n. 2, pp. 182–197.

[30] Barbosa, H. J. C. & Lemonge, A. C. C., 2002b. An adaptive penalty scheme in genetic algorithms for constrained optimization problems. In *GECCO*, volume 2, pp. 287–294.

[31] Nicoară, E. S., 2007. Performance measures for multi-objective optimization algorithms. *Buletinul Universităţii Petrol–Gaze din Ploieşti., Seria Matematică-Informatică-Fizică*, vol. 59, n. 1, pp. 19–28.

[32] Deb, K., 2001. *Multi-objective optimization using evolutionary algorithms*, volume 16. John Wiley & Sons.

[33] Vargas, D. E. C., Lemonge, A. C. C., Barbosa, H. J. C., & Bernardino, H. S., 2015. Um algoritmo baseado em evolução diferencial para problemas de otimização estrutural multiobjetivo com restrições. *Revista Internacional de Métodos Numéricos para Cálculo y Diseño en Ingeniería*. (in portuguese).

[34] Fonseca, C. M. & Fleming, P. J., 1996. On the performance assessment and comparison of stochastic multiobjective optimizers. In *International Conference on Parallel Problem Solving from Nature*, pp. 584–593. Springer.

[35] Grunert da Fonseca, V., Fonseca, C., & Hall, A., 2001. Inferential performance assessment of stochastic optimisers and the attainment function. In *Evolutionary multi-criterion optimization*, pp. 213–225. Springer.

[36] López-Ibánez, M., Paquete, L., & Stützle, T., 2010. Exploratory analysis of stochastic local search algorithms in biobjective optimization. In *Experimental methods for the analysis of optimization algorithms*, pp. 209–222. Springer.

[37] Carvalho, C. R., Lemonge, A. C. C., Carvalho, J. P. G., Hallak, P. H., & Bernardino, H. S., 2017. Performance analysis of a particle swarm optimization algorithm to solve multiobjective optimization problems. *XXXVIII Iberian Latin-American Congress on Computational Methods in Engineering - CILAMCE*. Florianopolis - SC, Brazil.

[38] Zitzler, E. & Thiele, L., 1999. Multiobjective evolutionary algorithms: a comparative case study and the strength pareto approach. *IEEE transactions on Evolutionary Computation*, vol. 3, n. 4, pp. 257–271.

[39] Zhang, Q., Chen, J. C., & Chong, P. P., 2004. Decision consolidation: criteria weight determination using multiple preference formats. *Decision Support Systems*, vol. 38, n. 2, pp. 247–258.

[40] Carvalho, J. P., Lemonge, A. C., Carvalho, É. C., Hallak, P. H., & Bernardino, H. S., 2018. Truss optimization with multiple frequency constraints and automatic member grouping. *Structural and Multidisciplinary Optimization*, vol. 57, n. 2, pp. 547–577.

[41] Souze, R. R., Miguel, L. F. F., Lopez, R. H., Torii, A. J., & Miguel, L. F. F., 2016. A backtracking search algorithm for the simultaneous size, shape and topology optimization of trusses. *Latin American Journal of Solids and Structures*, pp. 2922–2952.

[42] Rahami, H., Kaveh, A., & Gholipour, Y., 2008. Sizing, geometry and topology optimization of trusses via force method and genetic algorithm. *Engineering Structures*, vol. 30, n. 9, pp. 2360–2369.

[43] Vu, T. V., 2015. Weight minimization of trusses with natural frequency constraints. In *11th World Congress on Structural and Multidisciplinary Optimisation*.